

USE OF MUONIC X RAYS FOR TISSUE ANALYSIS*

James J. Reidy[†]
University of Mississippi
University, Mississippi 38677

Richard L. Hutson
Los Alamos Scientific Laboratory
Los Alamos, New Mexico 87544

Klaus Springer
Technical University of Munich
Munich, Germany

Summary

The muonic x ray spectrum resulting from negative muons stopping in tissue samples and tissue "equivalent" materials has been obtained. Relative muonic x ray intensities have been determined and an attempt made to correlate these intensities with atomic abundances in these materials. A comparison of the results for the various targets is presented. Limits of sensitivity for fluorine and calcium in these biological materials have been established.

Results are outlined which demonstrate the feasibility of obtaining data in the singles mode, that is, without a muon telescope. This will allow one in the future to use the higher muon beam intensities which will be available at LAMPF. In addition, the use of larger targets will be possible and the possibility of using focusing collimators to interrogate a specimen is likely.

I. Introduction

Before the initial development of meson "factories" the possibility of using muonic x ray for elemental analysis of tissue had been suggested^{1,2} as has the possibility of using muonic x ray intensity ratios to differentiate between normal and pathological (e.g. tumors) tissue.³ Although some investigators have obtained muonic x ray spectra from biological materials^{4,5} there had been no programmatic effort devoted to studying the feasibility of using the muonic x ray intensities for analysis of biological materials. However, a program of this type has been initiated at the Los Alamos Meson Physics Facility (LAMPF) and some of the preliminary results are reported here.

The results from negative muons stopping in seven targets are reported. These targets are 1) pig muscle, 2) pig liver, 3) pig fat, 4) tissue equivalent liquid, 5) Shonka plastic, 6) Spokas plastic and 7) calf liver. The two plastics are often used as tissue equivalent materials in dosimetry studies and have well defined composition. They are considered to be essentially identical materials. The tissue equivalent liquid is a composition which should closely resemble the elemental composition of muscle and also has a well defined composition.

II. Experimental Arrangement and Data Acquisition and Analysis

An arrangement shown schematically in Figure 1 was placed in the beam at the stopped channel of the Los Alamos Meson Physics Facility (LAMPF).

The energy of the incident beam was 110 MeV and the flux about 90×10^3 negative muons per second for a 6 μ amp proton beam. With the 6% duty cycle of the machine this gives an instantaneous flux of about $15 \times 10^5 \text{ sec}^{-1}$. At times the proton beam was increased which resulted in a 50% increase in these flux values. The contamination in the beam is less than 0.1% negative pions and about 2% electrons.

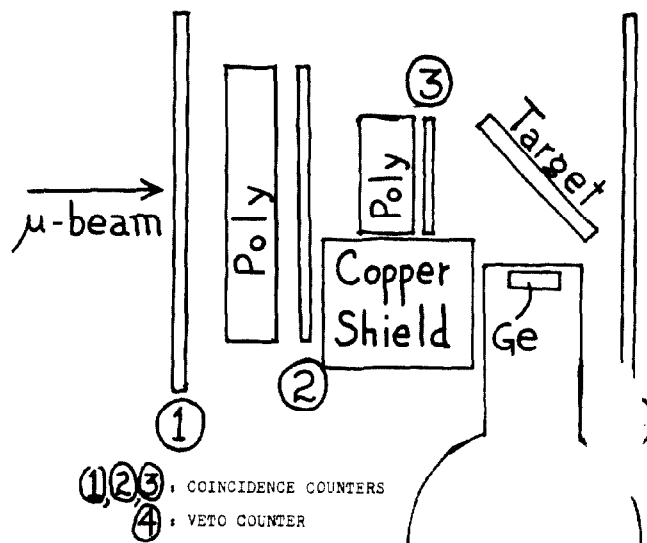


Figure 1. Experimental Arrangement

The targets each have a thickness of 2.0 gm/cm^2 and are 10 cm wide by 7.5 cm high. They are oriented vertically and 45° to the beam. This gives a target area perpendicular to the beam of 7.1 cm by 7.5 cm and a thickness of 2.8 gm/cm^2 parallel to the beam. The muon stop rate in the target, characterized by a 1234 coincidence requirement, was maximized by inserting a total of 11.5 cm of polyethylene in the beam. This gave an average stopping rate in the targets of about $4 \times 10^4 \text{ sec}^{-1}$. Scintillator 3 (Figure 1) has an area 7.5 cm x 7.5 cm thereby insuring that a muon passing through this scintillator will hit the target (except for the small fraction that may scatter). Scintillator 3 is set 5.5 cm from the center of the target and parts of it can be "seen" by the Ge detector. This results in a significant muonic carbon x ray contribution from muons stopping in this scintillator. By running a "dummy" target of beryllium (having a thickness of 2 gm/cm^2) the amount of this background (non-target) radiation was determined.

The germanium detector located 7.0 mm from the center of the target is an intrinsic device in the shape of a right circular cylinder with a diameter 35mm and a thickness 12mm. It is housed in a stainless steel cryostat with a 0.025 mm beryllium window. The resolution of the system was 800 eV at 122 keV.

* Work done under the auspices of the U.S. Atomic Energy Commission

† Work supported in part by a Faculty Research Grant from the University of Mississippi

A Canberra 8100 multichannel analyzer was used for data acquisition with subsequent storage on magnetic tape.

The targets were suspended in a styrofoam box which had provision for holding dry ice. This was necessary in those cases where we wished to keep the tissue targets frozen. In those cases where dry ice was used the non-target radiation was determined with the beryllium target and with the dry ice in place.

The fast coincidence system was of conventional design with a resolving time of 10 nsec. The signal from the germanium detector was amplified and put into a constant fraction discriminator. The output of this discriminator and of the fast coincidence system were used as inputs into a time-to-amplitude converter and a discriminator allowed one to select the coincidence timing range. A resolving time of 70 nsec resulted in a uniform range of coincidence from 15 keV to about 2 MeV. The coincidence efficiency was greater than 95%. The average count rate in the analyzer, characterized by a ^{123}I Ge coincidence requirement, was about 200 sec⁻¹ for the tissue targets. Some spectra were accumulated without the ^{123}I requirement and instead the analyzer was gated with a pulse obtained from the primary proton beam. The analyzer counting rate increased by about a factor of two in this case—primarily due to an increase in the background.

The x ray spectra were analyzed using the Los Alamos version of the gamma-ray analysis program GAMANAL¹. Background corrections were made using the data from the beryllium target runs and source absorption and detector efficiency corrections were applied.

TABLE 1. RELATIVE MUONIC X RAY INTENSITIES

ELEMENT	TRANSITION	INTENSITY-%
<u>Spokas Plastic</u>		
C	2p-1s	55
	3p-1s	20
	4p-1s	11
	5p-1s	3.3
	6p-1s	0.85
N	2p-1s	2.3
	3p-1s	0.76
	4p-1s	0.38
	5p-1s	0.24
O	2p-1s	3.7
	3p-1s	1.3
	4p-1s	0.94
	5p-1s	0.40
F	2p-1s	0.57
Ca	3d-2p	0.30
<u>TE Liquid</u>		
C	2p-1s	8.5
	3p-1s	3.5
	4p-1s	1.8
	5p-1s	0.87
N	2p-1s	2.2
	3p-1s	1.1
	4p-1s	0.34
O	2p-1s	4.8
	3p-1s	1.4
	4p-1s	1.2
	5p-1s	5.4
	6p-1s	1.8

III. Results

The intensity values for the muonic x rays from six targets are reported here. For two of these targets, Spokas plastic and a tissue equivalent liquid, the spectra have been analyzed in detail. The result of this analysis is presented in Table 1. The first column lists the element of interest, the second column designates the x ray transition, and the last column gives the measured relative x ray intensity. Including systematic errors the overall uncertainty in these values is estimated to be about 15%. However, within each elemental grouping the relative uncertainties are about 5%, except for the carbon series where source absorption corrections lead to a relative uncertainty of about 10%. The intensities are normalized so the total x ray intensity for each target is very nearly 100%.

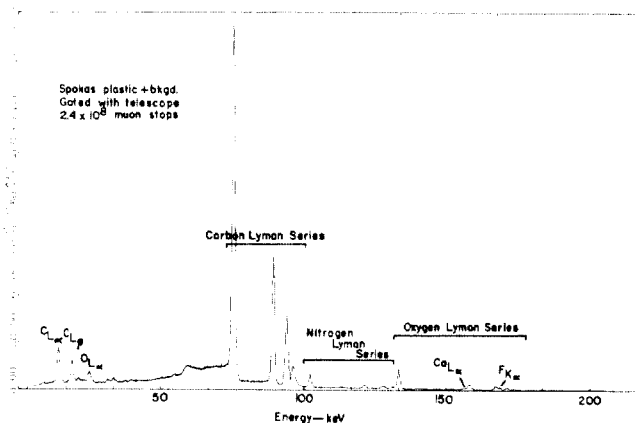


Figure 2. Spectrum from Spokas Plastic

The spectra obtained with the Spokas plastic target is shown in Figure 1. Besides the C, N, and O Lyman series lines the $F_{K\alpha}$ line is also evident. In addition, the analysis shows the presence of the Ca L_{α} line as well. Table 2 lists the energies of the muonic x ray lines of interest.

Table 2. MUONIC X RAY ENERGIES (keV)

ELEMENT	K_{α}	K_{β}	K_{γ}	K_{δ}	K_{ϵ}
C ^a	75.3	89.2	94.1	96.4	97.6
N ^a	102.4	121.4	128.1	131.2	
O ^a	133.5	158.4	167.1	171.1	173.3
F	168.2	199.7			
S	$L_{\alpha} = 100.7$		$L_{\beta} = 135.7$		
K	$L_{\alpha} = 142.6$		$L_{\beta} = 192.0$		
Ca	$L_{\alpha} = 158.2$		$L_{\beta} = 212.9$		

a) T. Dubler et al, Nuc. Phys. A 219 (1974) 29

Results for the calculated and measured relative total Lyman series x ray intensities for the Spokas plastic and tissue equivalent (TE) Liquid targets are given in Table 3. Column one lists the element and its atomic abundance in percent, column two gives the

calculated total intensity for each Lyman series (except hydrogen) based only on the atomic abundance, column three gives the calculated intensity assuming a Z-law correction², column four gives the calculated intensity assuming a "modified" Z-law correction, and column five lists the measured values.

In calculating the values for the intensities, we assumed that those muons which were initially captured by hydrogen are ultimately transferred to the heavier atoms. For the values in column two we assumed the number of muons transferred to each atom (heavier than hydrogen) was proportional to the number of heavier atoms present in the target (i.e. the atomic abundance). The values in column three were calculated assuming the number transferred was proportional to the atomic number of the atom (i.e. capture predicted from the simple Z-law). The Fermi-Teller Z-law states that the relative number of muon captures in an element will be proportional to the atomic number of the element. For the values obtained in column four, we assumed that the muons were initially captured in proportion as predicted from the Z-law - this includes capture in hydrogen. However, we further assumed that the muons would be transferred from hydrogen to the nearest heavy atom irrespective of its Z-value. This calculation necessitated a knowledge of the molecular form of the target.

TABLE 3. TOTAL LYMAN SERIES MUONIC X RAY INTENSITIES

Element- Atomic %	Relative Total Lyman Series Intensities			Measured ^a
	Calculated			
	No Z-law	Z-law	Modified Z-law	
<u>SPOKAS PLASTIC</u>				
H-58.75				
C-32.85	79.6	74.1	88.7	89.1
N- 3.65	8.8	9.6	4.9	3.7
O- 3.65	8.8	11.0	4.9	6.3
F- 0.74	1.8	2.5	1.5	0.9
<u>TE LIQUID</u>				
H-63.47				
C- 6.35	17.4	7.35	14.7	14.7
N- 1.56	4.3	4.21	5.0	3.6
O-28.38	77.9	87.6	80.3	81.7
S- 0.06	0.16	0.37	-	-
K- 0.06	0.16	0.46	-	-

a)Uncertainties about 10%

Table 4 presents the results of the measurements on the six targets reported here.

TABLE 4.
MEASURED RELATIVE TOTAL LYMAN MUONIC X RAY INTENSITIES^a

TARGET	RELATIVE INTENSITIES		
	C	N	O
Spokas Plastic	90	3.7	6.3
Shonka Plastic	89	4.3	6.7
Pig Fat	50	9.8	40
Pig Muscle	19	2.6	78
Pig Liver	15	2.6	82
TE Liquid	14.7	3.6	81.7

a) Uncertainties about 10%

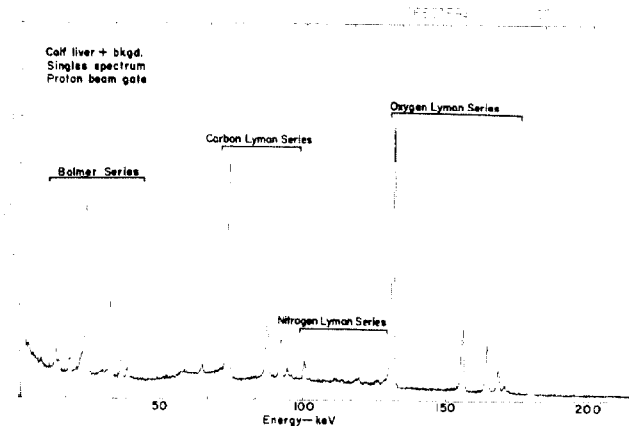


Figure 3. Singles Spectrum from Calf Liver

Figure 3 shows the spectrum resulting from using a calf liver target and gating, not with the muon telescope, but using the macropulse of the primary proton beam (6% duty cycle). The experimental arrangement was identical to that shown in Figure 1.

IV. Conclusions

Although the muonic x ray tissue analysis program is in its formative stages, some important results have already been obtained. From the values shown in Table 1, one finds that the ratios of line intensities for a given element in different compounds are not always the same. For example, the O(2p-1s)/(3p-1s) ratio for the Spokas plastic is 2.85 whereas it is 3.43 for the TE Liquid. The N(2p-1s)/(3p-1s) ratio for the Spokas plastic is 2 whereas it is 3 for the TE Liquid. Consequently, it appears that the chemical form of the target can affect the individual line intensities. This effect has been observed by others and is discussed in reference 9. Ultimately, this may allow one to differentiate among tissue samples by using such ratios as signatures. For example, this could lead to the ability to differentiate among normal tissue, malignant tumors and benign tumors.

Chemical effects in the muonic capture process

are also indicated by the results presented in Table 3. If the muon capture rate depended only on the number of atoms present then one would expect a correlation between the total Lyman series intensity and atomic abundances. This follows since each captured muon ultimately reaches the 1s state. Likewise, a correction for the Z-value of the atom might be expected to give intensity ratios correlated with column 3. However, the measured intensity values are in closest agreement with the calculated values obtained with the "modified" Z-law approach. Inherent in this calculation is a correction to the intensities arising from the molecular structure of the target. Although the approach is similar, this correction is not necessarily the same that one would obtain by assuming that a large fraction of muons is captured into molecular orbitals. From the data in Table 3, it appears that one may be able to establish a correlation between the muonic x ray intensities and atomic abundances provided some information is available about the molecular structure of the target; conversely, one may be able to use the x ray intensities in the study of molecular structure in biological samples.

Also, if the capture process for negative muon is similar to that for the negative muons, then the data shown in Table 3 indicate that a correction similar to the "modified" Z-law approach may be necessary in performing muon dosimetry calculations.

The results shown in Table 4 indicate that, as expected, the Spokas and Shonka plastics give similar results. The decreased water content in fat is evident from the lowered oxygen intensity as compared to muscle or liver. The carbon/oxygen intensity ratio for the fat, muscle and liver is 1.25, 0.18 and 0.24 respectively. These can compare to similar measurements on pig fat, horse muscle and calf liver performed by Daniel et al. where they obtained ratios of 4.59, 0.36 and 0.32 respectively. In addition, for the $N(2p-1s)/O(2p-1s)$ intensity ratio Daniel et al. obtained values of 0.043, 0.026, and 0.033 for the pig fat, horse muscle and calf liver, respectively. The corresponding values for the fat, muscle and liver samples reported here are 0.245, 0.032 and 0.033. A great deal of further study is needed before one can interpret these contrasting results.

The spectrum shown in Figure 3 illustrates that it is feasible to obtain data without a beam telescope - even in the Balmer series region. This will allow irradiations at higher beam intensities without the attendant high count rate problems. This will enable one to interrogate smaller target volumes (giving greater homogeneity in the case of tissue samples) and to use shorter counting times. A larger number of targets can be investigated and possible systematic effects noted. This is being actively pursued.

The threshold sensitivity of the present technique using the 10 cc Ge detector for F and Ca appears to

be about 0.3% atomic abundance in targets with appreciable amounts of oxygen. A larger detector and/or tighter geometry could decrease this threshold sensitivity by an order of magnitude.

The lines in the Balmer series are evident in all our spectra and may prove to be helpful in studying the surface layers of biological materials. These x rays are rapidly attenuated by tissue and the detected x rays originate dominantly from the first millimeter or so of tissue. The possibility of using the singles spectra (Figure 3) to obtain these intensities eliminates the need for a low energy coincidence range. The rapidly increasing background at these low energies can be modified by suitable collimators and other geometrical improvements. This is also being investigated.

Acknowledgments

The authors wish to thank Dr. M. Schillaci for his assistance in computing the target absorption corrections and A. Chavez for his invaluable assistance in the GAMANAL analysis.

We benefited a great deal from many helpful discussions with Prof. H. Daniel and he and Prof. H.B. Knowles provided much needed assistance during the experiments. Without the encouragement and assistance of Dr. L. Rosen much of this work would have been impossible.

Finally, we wish to express our appreciation to the LAMPF operations staff for their untiring efforts.

References

1. H. Daniel, Nucl. Med 8 (1969) 311
2. L. Rosen, Science 173 (1971) 490
3. J.J. Reidy, Los Alamos Report LA-5300-MS, pg. 37
4. H. Daniel, H.-J. Pfeiffer and K. Springer, Biomed. Technik 18 (1973) 222
5. M.C. Taylor, L. Coulson and G.C. Phillips, Rad. Res. 54 (1973) 335
6. N.A. Figario et al., Phys. Med. Biol. 17 (1972) 792
7. R. Gunnik and J.B. Niday, UCRL-51061 (unpublished)
8. E. Fermi and E. Teller, Phys. Rev. 72 (1947) 399
9. L.I. Ponomarev, Ann. Rev. Nucl. Sci. 23 (1973) 395